International Journal of Disaster Risk Reduction 91 (2023) 103668

Contents lists available at ScienceDirect

International Journal of Disaster Risk Reduction

journal homepage: www.elsevier.com/locate/ijdrr

Effect of retrofit interventions on seismic fragility of Italian residential masonry buildings

Veronica Follador, Pietro Carpanese *, Marco Donà, Francesca da Porto

Department of Geosciences - University of Padova, Via G. Gradenigo 6, 35131, Padova, Italy

ARTICLE INFO

Keywords:
Residential masonry buildings
Seismic vulnerability
Seismic retrofit interventions
Mechanical fragility model
Large scale analyses

ABSTRACT

In this paper, the vulnerability of ordinary unreinforced masonry (URM) buildings is analyzed, and the literature related to possible seismic retrofit interventions is reviewed in order to investigate their feasibility and effectiveness. These interventions are then simulated on a database of 445 buildings through *Vulnus_4.0* software, that performs simplified mechanical analyses accounting for both global and local behavior of masonry buildings. The fragility of each building is assessed both in its as-built state and after the simulation of retrofit interventions. Fragility curves are then processed, and a fragility model for four building typologies is obtained for the as-built and the seismic retrofitted configurations. Lastly, mean damage maps are elaborated, and the performance of the proposed retrofit interventions is analyzed. The results of this work allow evaluating and comparing the improvement of seismic behavior brought by various retrofit interventions and could serve as a basis for further theoretical studies and for practical design in real cases.

1. Introduction

The seismic events occurred in Italy during the last decades have shown the high vulnerability of the residential built heritage, which is mainly composed by historical buildings not seismically designed. Several national [1–4] and international [5–7] studies based on direct field observations of post-earthquake damage demonstrate a lack of capacity of old masonry buildings to resist to horizontal actions. Notwithstanding, both masonry and reinforced concrete (RC) buildings suffered high damage. The damage suffered by RC buildings is often associated to non-structural elements (i.e., extensive cracking and ejection of infill walls), although also collapses due to story mechanisms caused by the shear failure or flexural yielding at end sections of columns have been observed [8]. On the other hand, unreinforced masonry (URM) buildings usually experienced more severe damage levels [4,9], exhibiting both in-plane and out-of-plane failure mechanisms. This behavior is due to a lack of adequate connections and structural details, low mechanical characteristics of the masonry material and structural irregularities. Moreover, masonry disaggregation has often been observed in case of poor masonry and mortar quality [1]. Conversely, good seismic performances have been observed in modern masonry buildings, most of which showed negligible damage or suffered limited shear damage, in the form of diagonal and bi-diagonal cracks at the ground floor. This is due to the adequate masonry quality and the regular structure with rigid and well-connected diaphragms, which provide significant shear redistribution among walls and overstrength [3,4].

The serious damage caused by earthquakes keeps leading to many casualties and huge amount of economic losses. This issue has

* Corresponding author.
E-mail addresses: veronica.follador@unipd.it (V. Follador), pietro.carpanese@phd.unipd.it (P. Carpanese), marco.dona1@unipd.it (M. Donà), francesca.daporto@unipd.it (F. da Porto).

https://doi.org/10.1016/j.ijdrr.2023.103668
Received 23 November 2022; Received in revised form 23 March 2023; Accepted 28 March 2023
Available online 31 March 2023

motivated several studies aimed at defining the vulnerability of the building typologies diffused in Italy, to better understand the seismic risk at a territorial level and make it possible to plan seismic risk mitigation strategies at national scale. An example is the updating of the national assessment of disaster risk [10], developed by the Italian Department of Civil Protection (DPC) in response to the recommendations of the Sendai Framework for Disaster Risk Reduction 2015–2030 [11]. The document, called "National Risk Assessment", contains an overview of potential major disasters in Italy, including a contribution related to the seismic vulnerability assessment of the Italian residential building heritage.

In this context, the scientific community, in particular ReLUIS (Italian Network of the University Laboratories of Seismic and Structural Engineering) and Eucentre (European Center for Training and Research in Earthquake Engineering) have been working on the development of large-scale seismic vulnerability and fragility models related to specific macro-typologies of buildings, distinguished by age of construction, type of load-bearing structure (i.e., RC and masonry) and height classes [12,13]. In those works, six fragility models were developed, derived by means of mechanical models [14,15], using empirical approaches [16–18], or empirical-heuristic methodologies [19]. In the literature, it is possible to find many other methods for assessing both large-scale and building scale seismic vulnerability [20–23], but the above-mentioned approaches are very well suited to applications at territorial scales thanks to the definition of macro-typologies of buildings on the basis of available census data [24].

After developing seismic vulnerability analyses of the existing built heritage, the scientific community has started investigating the effectiveness of single retrofit interventions or extensive risk mitigation strategies [25–27]. To do this, the impact of possible retrofit interventions on risk mitigation must be estimated. This issue was addressed within a ReLUIS project called MARS (MAppe di Rischio Sismico – Seismic Risk MAps), developed in 2019–2021, and continues today within the MARS2 project 2022–2024 [28]. Indeed, a specific task of these projects includes the development of mitigated fragility sets taking into account different seismic retrofit interventions, to carry out mitigated risk analyses and thus evaluate the effectiveness of different strategies.

The purpose of this paper is to present retrofitted fragility curves, developed within the above-mentioned ReLUIS projects, simulating different types of interventions on a database of residential masonry buildings. Those buildings have been already analyzed in their as-built condition in previous studies [14,29,30]. This elaboration allows estimating the vulnerability reduction brought by different retrofit interventions, and it gives an indication of their effectiveness when applied at a large scale.

2. Macro-typologies of buildings and seismic retrofit interventions

The database selected to carry out the analyses is composed of 445 residential masonry buildings belonging to four macro-typologies, according to their construction period. The four macro-typologies include: a) historical buildings designed before 1919; b) buildings designed between 1919 and 1945; c) buildings designed between 1946 and 1960; d) buildings designed between 1961 and 1980. More modern buildings, i.e., those designed after 1980, have been excluded from this study since they usually show high quality construction details and have been built following more recent design codes. For these reasons, they are less vulnerable according to fragility analyses (e.g., Refs. [14,17–19]) and can be considered adequate enough to withstand seismic actions, as also demonstrated by recent post-earthquake surveys [3,4]. Indeed, the first specific regulation for the calculation of masonry structures, that introduced requirements on the construction details and geometry of masonry buildings, entered into force thanks to the Italian Ministry of Infrastructures in 1987 [31]. Therefore, those buildings in general do not require specific retrofit interventions, unless they have specific deficiencies.

Each macro-typology defined by age is then divided into 2 sub-typologies defined by height: Low-Rise (LR) buildings (1 or 2 stories), or Mid-Rise (MR) buildings (more than 2 stories, i.e., 3, 4 or 5 stories).

In general, the subdivision has been defined based not only on factors that influence the vulnerability of the building (i.e., building height and construction techniques), but also on the Italian national census [24], the most complete national building stock dataset available in Italy. The main criteria considered for the sampling of the buildings collected to perform the fragility analysis and the database itself have already been extensively described in Donà et al. [14]. The case studies were selected on the basis of typological and geographical representativeness from several sources. About 50% of the database consists of surveys directly carried out by the research group of the University of Padova in recent years, whereas the remaining part is composed of projects of public housing or private buildings published on books or kindly provided by architects, engineers and municipal offices. The distribution of the analyzed sample is shown in Table 1 by construction period and height class and some examples of buildings that were collected in the database are shown in Fig. 1

Once the building macro-typologies are defined, it is necessary to identify which retrofit interventions can be considered feasible and meaningful for each of them. To do so, the main characteristics of each macro-typology have been investigated in terms of materials, construction details and building techniques. Information about these features has been collected from Italian construction standards, technical architecture manuals, and other projects, previously examined and extensively presented in Ref. [14]. The main typological parameters that are considered significant for this work are summarized in Table 2. Pre-1919 and 1919–1945 typologies are very similar, with most buildings made of stone or solid brick masonry, wooden floors without ring-beams, and sometimes with

Table 1
Distribution of case studies in the database.

	Pre 1919	1919–1945	1946–1960	1961–1980
LR (*1-2 stories)*	70	53	43	58
MR (*3-5 stories)*	135	27	37	22

Fig. 1. Examples of Italian masonry buildings by construction period and height class.

tie-rods acting as wall-to-wall connections. In the mid 1940s, new construction technologies began to spread: stone and solid bricks were gradually replaced by hollow bricks, and floors started to be composed almost exclusively of reinforced concrete (RC) and hollow-tile blocks, with the presence of ring-beams at every floor, despite the fact that ring-beams built before the late 1980s are often not adequately reinforced.

3. Methodology

3.1. *Vulnus_4.0 software*

The software used to carry out mechanical analyses of each building of the dataset is *Vulnus_4.0*, developed at the University of Padova from 1990 [32] and subsequently updated in 2010 [33], up to the current 2022 web version (https://vulnus.dicea.unipd.it/ [34]). *Vulnus_4.0* analyzes load-bearing masonry structures in a simplified way. Through limited information about geometry (plan and elevation layout), material properties, construction details, and qualitative information, the software estimates the resistance of the load-bearing masonry wall system of a building in its two main directions to out-of-plane (OOP) mechanisms and in-plane (IP) shear stress, in order to assess a general vulnerability level of the building. In particular, three indices are calculated.

The first index *I1* is computed as the minimum IP shear failure critical acceleration (normalized to gravity acceleration g) of the two main parallel wall systems of the building, and is then normalized to the gravity acceleration *g*.

The second index *I2* represents the calculated critical acceleration (also normalized to g) that causes the activation of the main OOP collapse mechanisms. The triggering acceleration is calculated for each wall and for several mechanisms, including: the overall overturning of the wall, the overturning and flexural failure of the top story, the flexural and the arching mechanism failure at the last story, the overturning and the flexural collapse of the arch shoulders at the last story, and the detachment of the transverse walls at the last story.

Lastly, the *I3* index provides a vulnerability evaluation based on qualitative features of the building not included in the other two indices. It is calculated using the scores assigned to 11 qualitative parameters collected in the GNDT "Second Level" form [35]. Specifically, a class from A to D (where A is the best condition) is assigned to every parameter and is then associated to a numerical score.

The software performs a vulnerability analysis based on these three indices using the fuzzy sets theory [36]. In particular, *Vulnus_4.0* provides estimates of the expected seismic damage in the form of three fragility curves expressed in Peak Ground Acceleration (PGA). The three curves represent a medium-severe damage state (assumed as a DS2-3 of the European Macroseismic Scale EMS98 [37]), and they are defined as a "White" curve, that represents the average building vulnerability, a "Lower-Bound" curve and an "Upper-Bound" curve, that represent the extreme probabilities and define a range of vulnerability due to the various sources of

Table 2
Summary of typological information for each construction age.

	Pre-1919	1919–1945
Material	Stones or solid bricks	Solid bricks or stones
Floor type	Wood	Wood, precast RC or hourdis hollow-tiles
Ring-beams	Missing	Missing, or poorly reinforced
Connections	Mostly ineffective, possible presence of tie-rods	Often ineffective, possible presence of tie-rods
	1946–1960	***1961–1980***
Material	Solid bricks or hollow bricks	Hollow bricks
Floor type	RC and hollow-tiles	RC and hollow-tiles
Ring-beams	At every floor, poorly reinforced	At every floor, not adequately reinforced
Connections	Often ineffective	Sometimes ineffective

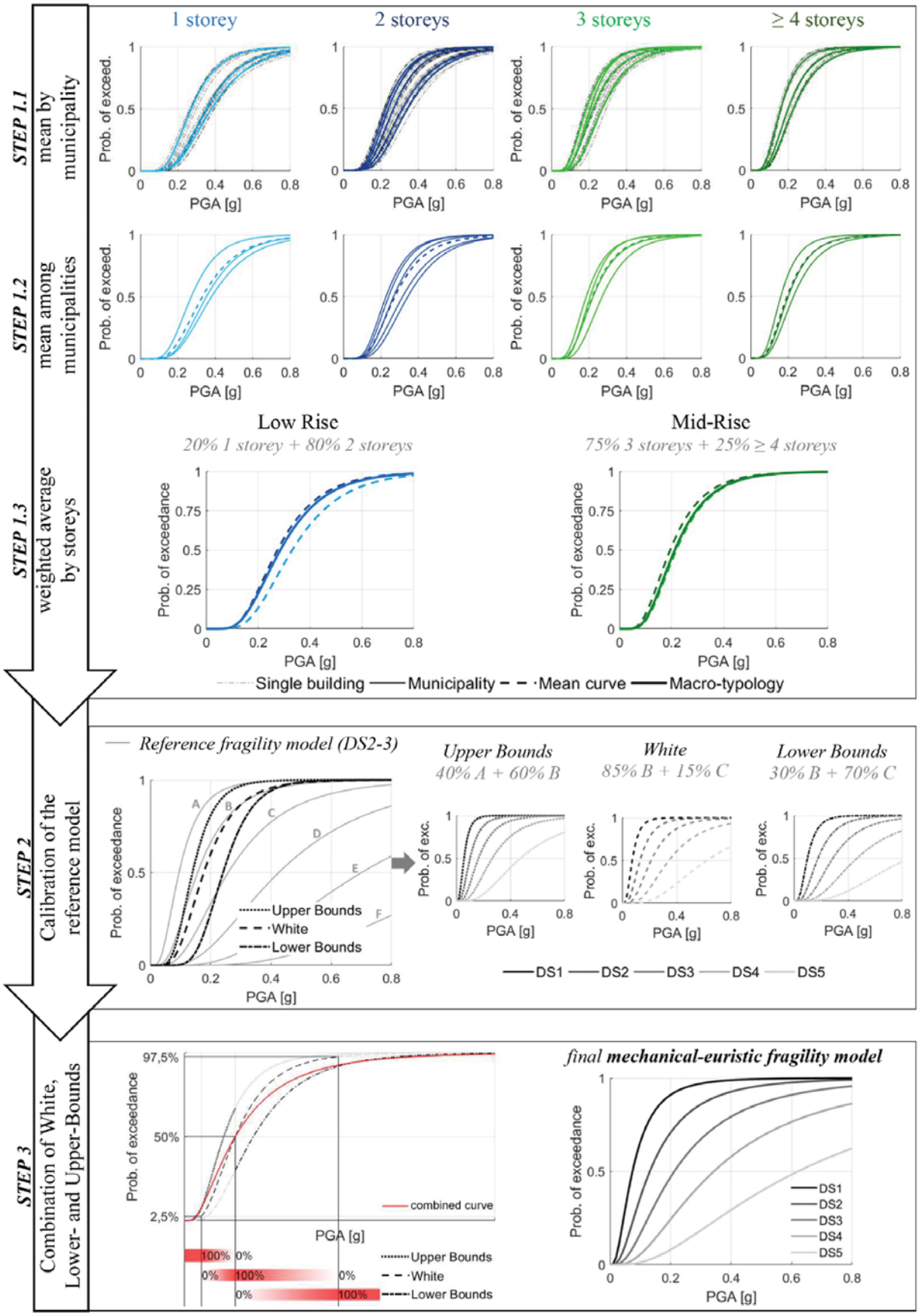

Fig. 2. Procedure of post-processing of the *Vulnus_4.0* results (modified starting from Donà et al. [14]).

uncertainty (i.e. mechanical properties of the material, geometry regularity both in plan and elevation, effectiveness of construction details, etc.). Indeed, especially when using a simplified procedure to produce fragility curves, it is essential to take model uncertainties into account, such as the possible variability of construction parameters and the quality and reliability of the data [38–40].

Further information on how the software computes each index and the fragility curves can be found in Refs. [29,33,34].

3.2. Methodological approach

The curves produced by *Vulnus_4.0* are calculated for discrete PGA values, but can be fitted with continuous cumulative lognormal distributions, which are often used to describe the seismic fragility of buildings. Lognormal fragility curves are described by two parameters: the median value μ of the intensity measure (PGA) of a specific damage state (DS), and the standard deviation β describing the dispersion. These two parameters have been defined, for each building, through the application of the maximum likelihood method to the discrete curves obtained through *Vulnus_4.0*.

The following is an overview of the procedure of post-processing of the *Vulnus_4.0* results (Fig. 2), carried out to develop the complete final set of fragilities, whose extensive description and validation can be found in Donà et al. [14].

- Step 1. For each macro-typology, the curves of each building with the same number of floors and age of construction are averaged first by municipality (Step 1.1 and 1.2 of Fig. 2), in order to maintain a geographical and typological representativeness. Then, the resulting fragility curves that describe buildings with a specific number of stories are averaged (Step 1.3 of Fig. 2) in order to obtain the height sub-class curve, considering for each sub-typology the actual real distribution obtained from ISTAT (2011) census data [24].
- Step 2. Since the curves produced by *Vulnus_4.0* represent a single damage state (DS2-3), they do not allow a complete interpretation of damage. In order to represent seismic fragility over five damage states (from DS1 to DS5, as described in EMS98), the macroseismic fragility model of [41] is calibrated on the mechanical fragility model obtained for DS2-3 (Step 2 of Fig. 2). Specifically, the macroseismic model is converted from macroseismic intensity to PGA according to a correlation law [42], and is then calibrated on the optimal solution between the minimization of the absolute error between the curves, according to the least squares method, and the minimization of the relative error, expressed as the difference of positive and negative areas between the curves.
- Step 3. The first two steps of the procedure are applied separately for the curves White, Lower- and Upper-Bound, resulting in three new mechanics-based heuristic fragility models: the most probable (White), and two boundary probabilities (Lower- and Upper-Bound). Considering the aim of providing a fragility model suitable for large-scale risk assessments, a single fragility set for each building macro-typology is derived by combining White, Upper- and Lower-Bound fragility sets as shown in Step 3 of Fig. 2. These curves were first obtained by discrete points, and subsequently converted into lognormal curves by applying the criterion of maximum likelihood in the PGA range of interest, i.e., from 0 to 0.8 g. This operation allows to maintain the average fragility defined by the White curves, but at the same time to increase the dispersion parameter within the two extreme boundaries.

4. Seismic retrofit interventions

Before carrying out vulnerability analyses through *Vulnus_4.0*, retrofit interventions must be selected as the most significant and effective for each building macro-typology. To do this, the reference literature was taken into account together with direct field observations [9,43–46]. In particular, due to the typological similarities among buildings erected in time periods that are close to each other, two blocks of interventions were selected, one for the so-called "historical" buildings (i.e., built before 1945) and one for more modern buildings (i.e., built after 1945). Specifically, the interventions have been grouped into three categories, depending on the kind of improvement that they are supposed to bring: a) interventions to increase the strength and quality of masonry (MSN), b) interventions to improve the wall-to-wall and wall-to-floor connections and to guarantee the box-like behavior (TR, CR), and c) interventions to increase the stiffness of the horizontal diaphragms (FLR) [47,48]. These interventions can be applied individually or they can be combined to optimize their effectiveness. In Table 3, the interventions selected for the two building macro-classes are shown. Four possible interventions are proposed for the two macro-typologies of buildings designed before 1919 and between 1919 and 1945, combined in 4 different ways, for a total of eight possible interventions. On the other hand, the interventions selected for

Table 3
Selected retrofit interventions for different construction periods.

Before 1945	*individual interventions*	MSN1	1st stage of masonry strengthening (one intervention)
		MSN2	2nd stage of masonry strengthening (combined interventions)
		TR	addition of tie-rods
		FLR	stiffening of floors (light intervention)
	combined interventions	MSN1+TR	1st stage of masonry strengthening + addition of tie-rods
		MSN1+FLR	1st stage of masonry strengthening + stiffening of floors
		MSN2+TR	2nd stage of masonry strengthening + addition of tie-rods
		MSN2+FLR	2nd stage of masonry strengthening + stiffening of floors
After 1945	*individual interventions*	MSN	masonry strengthening (reinforced plaster)
		CR	addition of confining rings
		FLR	stiffening of floors (heavy intervention)
	combined interventions	MSN + CR	masonry strengthening + addition of confining rings
		MSN + FLR	masonry strengthening + stiffening of floors

buildings designed between 1945 and 1980 are three, and their possible combinations lead to a total of five possible strategies.

In the following paragraphs, a detailed explanation of the most common interventions summarized in Table 3 and of their implementation through *Vulnus_4.0* software is given, taking into account the significant differences between the macro-typologies and the specific features of every single building. Due to the simplified modelling procedures of the software, the implementation process can be divided into two parts. The first part relates to the interventions that can be implemented through the available software options and are generally connected to changes in the mechanical parameters. However, some of the interventions had to be implemented indirectly, reproducing their effect on the overall behavior of the building. The second part of the implementation process refers to the improvement of building features that impact on seismic performance, i.e., the qualitative parameters of the Second Level GNDT form. According to the *Vulnus_4.0* software description given in §3.1, a qualitative class from A to D is assigned to each one of the 11 parameters of the form in their original conditions. Subsequently, given the effects of each intervention, a higher qualitative class is assigned to the parameters affected by the specific intervention, with reference to the technical manual of the form [35].

4.1. Improvement of masonry quality and strength

To ensure a good seismic performance of a masonry building, the quality and state of preservation of masonry is of paramount importance. If masonry is not sufficiently strong and compact, the application of seismic actions leads to stone disaggregation or severe in-plane shear failure. Several techniques can be applied to improve the performance of masonry, depending on the typology and quality of masonry itself [49], as also demonstrated by recent post-earthquake field observations [44]. Therefore, a careful evaluation of the as-built state of masonry is necessary to select the most suitable intervention.

As presented in Table 3, two stages of retrofit interventions on masonry are proposed in case of historical buildings (MSN1, MSN2), while only one stage is taken into consideration in case of modern buildings (MSN), because of their better as-built performance. The first stage of masonry intervention on historical buildings (MSN1) considers the application of lighter or single strengthening techniques, whereas the second one (MSN2) implies the concurrent application of two techniques or the extensive implementation of a heavier single technique, to achieve the best retrofit result.

The techniques used to improve the quality and strength of masonry proposed in this study vary according to the type of masonry. For what concerns historical buildings, the load-bearing structure is usually composed of stone or solid brick masonry. Specifically, the first usually consists of rubble stones with irregular patterns and presence of many voids, or of better shaped and coursed stone, the latter being generally of higher quality and more performing than the previous. Brick masonry is generally more regularly coursed. Both stone and brick masonry can be composed of two or three leaves, that are often not properly connected, particularly in the case of rubble, multi-leaf, stone masonry. Conversely, modern load-bearing masonry buildings (built after 1945) are generally made of industrialized solid or hollow bricks and blocks or, to a smaller extent, better shaped stones.

In case of inconsistent random stone masonry, grout injections are one of the most common and effective interventions [50–52]. This technique consists of grouting the wall core by filling the voids through a regular pattern of drilled holes. Nowadays, natural hydraulic lime-based grouts are usually preferred, as their composition is more similar to that of historic mortars, thus ensuring a better homogenization with existing materials [50,53,54].

Nonetheless, even in masonry composed of more regular elements (i.e., stone ashlar and solid brick), the mechanical characteristics (compressive and tensile strength) may need to be improved. On both regular stone and brick, and irregular stone masonry typologies, reinforced concrete jackets made of cement or lime-based mortars and welded steel meshes can be added ([55], Fig. 3a). Conversely, an intervention technique more suitable for masonry characterized by even surfaces and regular textures consists of FRP (Fiber Reinforced Polymer) and SRG (Steel Reinforced Grout) applications (Fig. 3b and c) consisting of strips made of glass, carbon, aramid, or polypropylene fiber meshes applied with either organic or inorganic matrixes [56–60]. FRCM-TRM (Fiber Reinforced Cementitious Mortar – Textile Reinforced Mortars) plasters represent an evolution of the previously described interventions. FRCM-TRM plasters consists of fiber meshes, coated in inorganic matrices based on lime or cement mortar and spread to the entire surface of the walls. The final

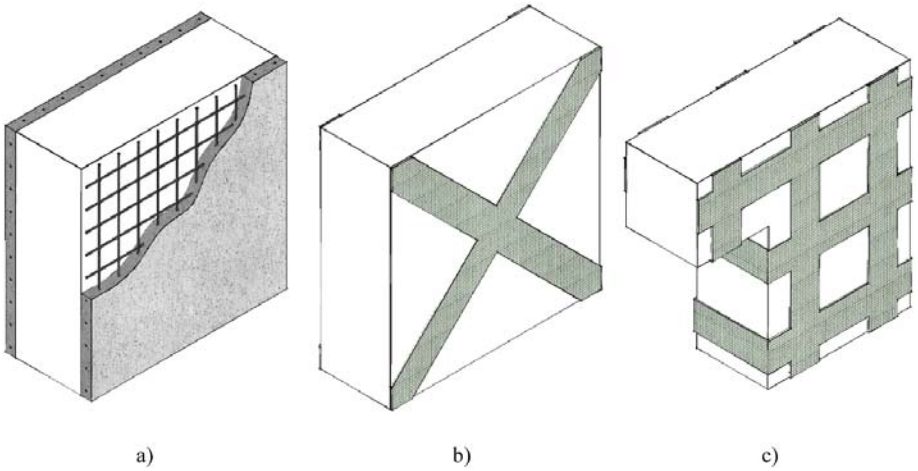

Fig. 3. Reinforced concrete jackets (a) and example of application of FRP-SRG (b, c).

outcome is similar to that of reinforced concrete jackets, but it comes with a lighter load, and in particular stiffness, increase. These reinforced plasters should be applied on both sides of the wall, although less performing one-side solutions, properly anchored by transversal connections, are also allowed [61–67]. This type of intervention is suitable also for more modern buildings, characterized by more regular masonry, where it is not necessary to fill internal voids, avoid masonry disaggregation, or improve the bond among different masonry leaves, but it is generally needed to produce a light but widespread strength increase.

The most suitable intervention in case of masonry with multiple leaves not adequately connected to each other is the insertion of artificial transverse elements with an anti-expulsion function, which can be applied only if the masonry is consistent enough to ensure the coupling between the faces, thus the overall functioning of the wall [68,69].

Lastly, when the resistant elements are mostly regular and performing, but the mortar is of very poor quality or in a deteriorated state, it is possible to act with bed-joint repointing [70], which could be also reinforced or not with steel or FRP bars [50,71].

To summarize, the 1st stage masonry interventions proposed in this study, according to the type of masonry, are injections on random multi-leaf stone, and the application of reinforced plaster or FRCM-TRM in case of stone ashlars, solid and hollow brick masonry. These interventions can be integrated, as 2nd stage intervention, with bed-joint repointing or reinforced bed-joint repointing (in case of regularly coursed masonry) and transversal connection elements (in case of multi-leaf stone masonry).

To simulate these types of intervention through *Vulnus_4.0*, the corrective coefficients shown in Table 4 are applied to the mechanical characteristics of the materials composing the building. The coefficients are averaged on those of table C8.5. II available in the Italian Circular 2019/01/21 [48], and depend on the type of intervention and on the construction material. In case of historical masonry, the first step of intervention brings a similar improvement for different masonry types. Instead, the implementation of more invasive and heavy interventions on stone masonry, characterized by values of the mechanical parameters lower than the ones associated to brick masonry, gives greater improvements, although it does not exceed the values of the mechanical characteristics of brick masonry. Moreover, the improvement in case of hollow brick masonry is very low, since the performance level in the as-built state is already high. Lastly, since these interventions require addition of material, an average increase of masonry specific weight was estimated by 5% in case of stone masonry and 4% in case of solid and hollow brick masonry.

As concerns the modification of the class assigned to the GNDT qualitative parameters, the improvement of masonry quality is related to four parameters: parameter n.1 “type and organization of the resistant system”; parameter n.2 “quality of the resistant system”; parameter n.3 “conventional resistance”; and parameter n.11 “state of preservation”. The parameters n.1 and n.3 are excluded from the calculation of the qualitative index I3 by *Vulnus_4.0* because the former is completely integrated in the OOP index I2, and the latter in the IP index I1 [33]. For this reason, only parameters n.2 and n.11 have been modified after the strengthening interventions. The parameter n.2, “quality of the resistant system”, depends on the homogeneity of the wall fabric, and it is assigned to an A class for particularly good masonry structures, or in presence of masonry consolidated according to current seismic standards [35]. The class of parameter n.2 has been thus changed to A either for MUR1, MUR2 and MUR, regardless of the as-built masonry type and original quality class. Parameter n.11 is classified based on the maintenance state of the masonry, and an A class is assigned to masonry in good condition, without visible damage, which can be also obtained after a well realized strengthening intervention. Therefore, also the class of parameter n.11 has been changed to A after the application of interventions.

4.2. Improvement of connections and box-like behavior

Connections between structural elements are necessary to ensure a box-like behavior of masonry buildings, which is the ability to act as an ensemble of all structural components, activating the in-plane response of the walls and resulting in a higher resistance of the structure to the horizontal actions caused by an earthquake.

Wall-to-wall and wall-to-floor/wall-to-roof connections are often inadequate in ancient buildings [44,45], causing a poor distribution of the shear loads in the masonry walls and the possibility of activating out-of-plane collapse mechanisms.

Interventions to improve wall-to-wall connections can be implemented by masonry corner reconstruction or by inserting steel or composite elements locally [72]. Interventions to improve the wall-to-floor connections can be carried out, for example, by inserting inclined steel bars in grouted holes drilled in the masonry, or by inserting fasteners (for example steel plates) at the ends of the beams, anchored on the external face of the wall or injected in holes in the wall [5,73–75]. The latter solution is particularly efficient in case of wooden floors (Fig. 4).

The most traditional and popular solution to obtain a box-like behavior is the insertion of steel tie-rods (TR) or confining rings (CR) [47,55,76–80]. TR are steel bars connecting parallel opposite walls, that allow preventing the out-of-plane overturning of walls and, when placed parallel to façade walls, allowing a better in-plane load redistribution and behavior of piers and spandrel walls (Fig. 5a). This technique is highly compatible, thus being one of the most traditional ones and very frequently implemented in historical

Table 4
Multiplicative coefficients applied by type of masonry and construction period.

Before 1945	MSN1	MSN2
Stone masonry	1.7	2.4
Solid brick masonry	1.5	1.8
Tuff masonry	1.6	1.9
After 1945	**MSN**	
Solid brick masonry	1.7	
Hollow brick masonry	1.3	

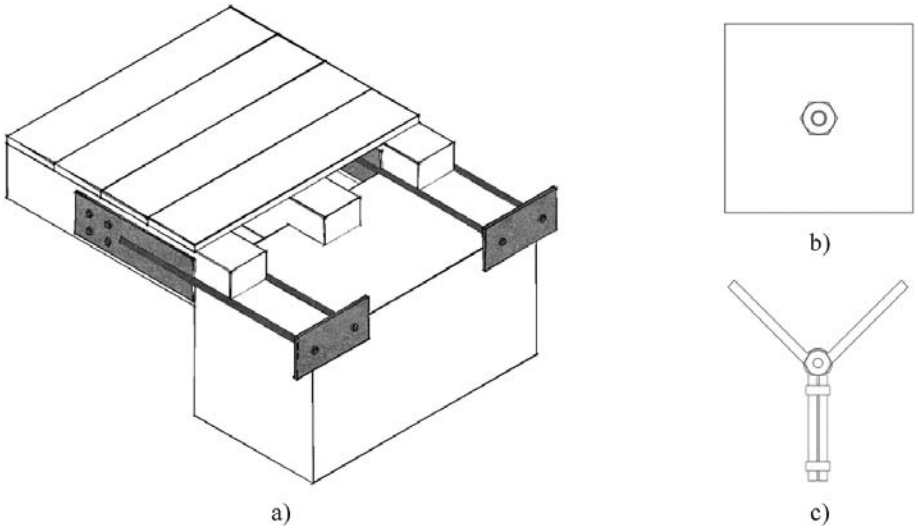

Fig. 4. Example of floor-to-wall connection (a) and of external anchors (b, c).

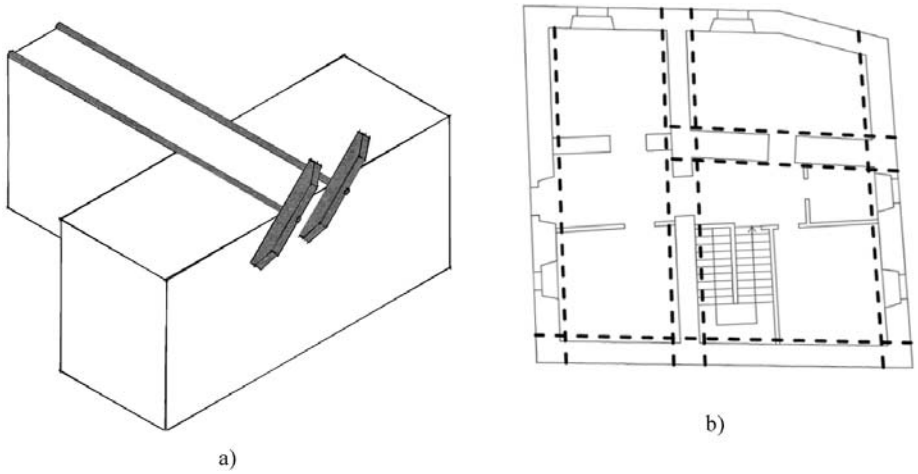

Fig. 5. Positioning of tie-beams: three-dimensional scheme (b) and position in plan (a).

buildings. Usually, TR are placed at floor level in conjunction with masonry corners or T-junctions, along external and internal load-bearing walls, in the two main directions of the building (Fig. 5b). TR can be directly implemented in *Vulnus_4.0*, that considers the presence of this type of element. The number of ties was calculated for each building by placing, along each main direction of the building, an adequate number of rods (two rods, one per side, placed parallel to the internal partitions, and one rod close to the perimeter walls).

As for the CR, these have the same function of TR, but they are applied on the external face of the walls. They consist of steel bars or bands of FRP/SRG placed all around the buildings [59,60,66]. The CR intervention has been considered as the equivalent of TR for modern buildings, useful when modern buildings are not provided with perimetral RC tie-beams or the RC tie-beams are insufficiently reinforced. The result of CR is indeed to counteract the OOP mechanisms of walls and to improve the overall box-like behavior of the building. In this case, as *Vulnus_4.0* does not explicitly consider the presence of this type of element, CR are simulated with the insertion of two TR in each direction, in correspondence of the horizontal diaphragms of the building.

For the intervention to be successful, both TR and CR need to be used when masonry is sufficiently compact and resistant to sustain the local force applied by the anchors. If this is not the case, it is necessary to apply local or global masonry strengthening interventions such as grout injections, reinforcement or replacement of individual degraded elements [67]. For the purpose of this study, this condition was considered to be originally verified (when only TR or CR interventions are applied), or to be satisfied with the application of a combined intervention, where a global masonry strengthening intervention is also foreseen.

The GNDT form takes into account the presence of these elements with particular reference to the issue of OOP thrusts at the roof level (parameter n.9 “roof”). According to the manual [43], the addition of tie-rods or other confining elements can improve the roof of one class. Consistently with the GNDT form, the implementation of TR or CR brings an upgrade of one class to parameter n.9.

4.3. Strengthening and stiffening of horizontal diaphragms

The horizontal diaphragms of masonry buildings have a crucial role on their seismic behavior, since they redistribute horizontal loads among load-bearing walls, thanks to sufficient stiffness and adequate connections to the vertical structure (load-bearing walls).

In general, there is a significant difference among the floor typologies in historical and modern buildings, resulting in different kinds of floor interventions (FLR) to be applied in the two cases. The horizontal diaphragms in ancient buildings often do not satisfy stiffness and connection conditions. Indeed, in this building typology it is common to find timber floors made with a single planking layer, usually not connected to the walls. In this case, interventions should aim at decreasing the in-plane deformability, and at strengthening the connections between horizontal structures and walls [81]. The floor intervention applied in this study, in case of historical buildings, considers the presence of wooden floors and consists in wooden planking reinforcement, which has proven to be very successful when applied to existing timber floors, as it helps increasing the in-plane stiffness without overloading [82–85]. This intervention consists of adding single or double wooden planks over the existing one, preferably using tongue-and-groove joints with nails or screws as connectors placed in orthogonal direction or at 45° (Fig. 6). Other strategies may be the insertion of diagonal metallic belts or composite material strips [86].

In case of modern buildings, floors are typically made of either reinforced lattice joist or steel beams and hollow tiles, and are usually completed with a concrete slab. The steel used as reinforcement is not always enough and, in particular, during the first evolutions of steel/hollow tiles and RC joist/hollow tiles floor systems, the connection between the joists and the slab was often inadequate or even absent, as well as the connections to the walls are often inadequate, due to the absence or poor reinforcement of RC tie-beams along the building [87]. In case of poor RC and hollow-tile floors, a concrete slab can be replaced or even added (Fig. 6b), with the insertion of adequate connections to the joists and to the walls around the building perimeter.

Regarding the implementation phase, *Vulnus_4.0* does not provide a way to implement intervention on the floors automatically, but it is necessary to simulate the effect of the intervention indirectly. Indeed, the implementation of the installation of double wooden planks in *Vulnus_4.*0 has been carried out by inserting ties to simulate the improved box-like behavior when floors are stiffened. Then, to further increase the reaction of the diaphragms in the model, the floor-to-wall friction coefficient is increased to take into account the improved connection brought by the intervention. For modern buildings, the replacement or the addition of the collaborating slab is simulated in *Vulnus_4.0* with the insertion of adequate connections with the walls around the entire perimeter. The floor-to-wall friction coefficient has not been increased, as in the historical buildings, since it already had non-negligible values due to the type of simulated floors, but tie-beams have been inserted at each floor, when they were not already present. By doing so, the insertion of tie-beams has not been considered as a stand-alone intervention, because of its difficult application, especially at the intermediate floor levels of historical buildings [43,44,88]. Also, an average increase of floor specific weight has been estimated by 1.2 kN/m^2, in case of newly added collaborating slabs.

The GNDT parameters concerned by the floor improvements are n. 5 “floor” and n.9 “roof”. The class of the parameter n. 5 is assigned based on the floor stiffness and the quality of the wall-to-floor connections. The interventions implemented in this study are attributed to an A or B class, based on the presence (class B) or absence (class A) of unaligned floors [35]. Instead, parameter 9 considers stiffness and quality of connections, but also the presence of thrusts, in case of heavy or light roofs. In this case, the intervention leads to an improvement of only one class, similar to what happens with TR and CR.

5. Mitigated fragility sets

The procedure presented in §3 has been repeated for each one of the 445 buildings included in the database designed before 1980 and analyzed in Donà et al. [14], for each intervention considered. As a result, the fragility sets related to the building macro-typologies Pre-1919, 1919–1945, 1946–1960, and 1961–1980, for the two height classes Low-Rise (1 and 2 stories) and Mid-Rise (3, 4 and 5 stories), are obtained. They are listed here in Table 5 and Table 6 in terms of median μ and standard deviation β of the lognormal cumulative fragility curve. The results are also graphically presented in Figs. 7 and 8, where the fragility sets of the retrofitted buildings (thick lines) are compared to those of the as-built (AB) ones (thin lines).

It must be borne in mind that the software *Vulnus_4.0* originally produces fragility curves only related to one specific damage state (DS2-3), from which a fragility set distributed over the five damage states is then derived. Therefore, the model obtained allows capturing the overall vulnerability reduction caused by the application of different interventions, but not the variations of individual

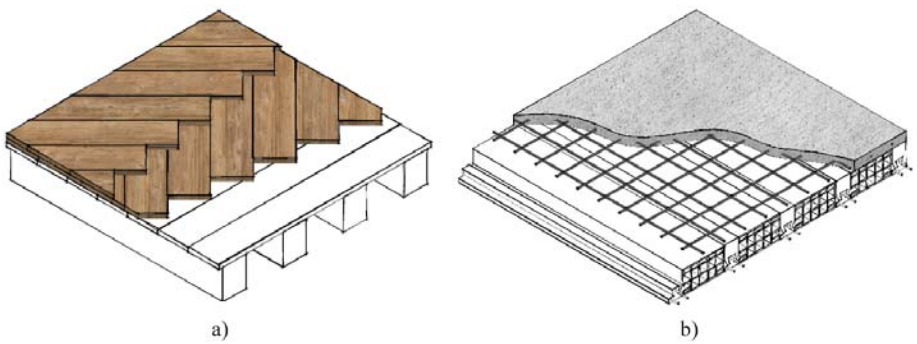

Fig. 6. Reinforced timber floor with double planking crossed at +45° and −45° (a) and addition of composite slab in RC floors (b).

Table 5
μ and β values of the as-built and retrofitted fragility models - historical buildings.

			DS1		DS2		DS3		DS4		DS5	
			μ [g]	β [−]	μ [g]	β [−]	μ [g]	β [−]	μ [g]	β [−]	μ [g]	β [−]
Pre-1919	AB	$n \leq 2$	0.098	0.693	0.173	0.715	0.280	0.718	0.453	0.751	0.825	0.793
		$n \geq 3$	0.073	0.747	0.129	0.776	0.209	0.784	0.337	0.781	0.612	0.808
	MSN1	$n \leq 2$	0.132	0.707	0.234	0.732	0.378	0.725	0.611	0.725	1.110	0.716
		$n \geq 3$	0.111	0.756	0.197	0.786	0.317	0.774	0.514	0.785	0.942	0.816
	MSN2	$n \leq 2$	0.154	0.694	0.274	0.726	0.442	0.735	0.715	0.758	1.301	0.684
		$n \geq 3$	0.127	0.748	0.225	0.780	0.363	0.767	0.587	0.772	1.068	0.767
	TR	$n \leq 2$	0.112	0.740	0.198	0.768	0.320	0.755	0.517	0.766	0.948	0.804
		$n \geq 3$	0.078	0.736	0.139	0.757	0.224	0.761	0.362	0.770	0.656	0.806
	FLR	$n \leq 2$	0.126	0.737	0.223	0.760	0.360	0.749	0.582	0.753	1.059	0.758
		$n \geq 3$	0.091	0.681	0.162	0.702	0.262	0.706	0.424	0.735	0.770	0.774
	MSN1+TR	$n \leq 2$	0.168	0.692	0.298	0.718	0.481	0.737	0.780	0.778	1.425	0.698
		$n \geq 3$	0.119	0.744	0.212	0.768	0.342	0.756	0.553	0.756	1.009	0.778
	MSN1+FLR	$n \leq 2$	0.205	0.702	0.365	0.703	0.588	0.683	0.945	0.677	1.685	0.670
		$n \geq 3$	0.148	0.671	0.262	0.694	0.423	0.699	0.684	0.717	1.241	0.672
	MSN2+TR	$n \leq 2$	0.190	0.730	0.338	0.737	0.545	0.729	0.879	0.761	1.579	0.711
		$n \geq 3$	0.142	0.701	0.253	0.729	0.408	0.733	0.659	0.747	1.196	0.697
	MSN2+FLR	$n \leq 2$	0.264	0.737	0.469	0.738	0.758	0.726	1.223	0.653	2.172	0.611
		$n \geq 3$	0.184	0.686	0.327	0.700	0.529	0.709	0.856	0.752	1.554	0.708
1919–1945	AB	$n \leq 2$	0.107	0.753	0.190	0.767	0.307	0.765	0.496	0.785	0.910	0.813
		$n \geq 3$	0.084	0.719	0.149	0.746	0.241	0.751	0.390	0.768	0.707	0.819
	MSN1	$n \leq 2$	0.142	0.705	0.253	0.733	0.408	0.742	0.660	0.764	1.197	0.712
		$n \geq 3$	0.118	0.784	0.209	0.814	0.338	0.802	0.547	0.802	0.999	0.809
	MSN2	$n \leq 2$	0.162	0.701	0.287	0.734	0.465	0.754	0.753	0.791	1.373	0.694
		$n \geq 3$	0.138	0.728	0.245	0.760	0.395	0.770	0.638	0.790	1.159	0.749
	TR	$n \leq 2$	0.116	0.771	0.206	0.798	0.332	0.781	0.538	0.774	0.983	0.803
		$n \geq 3$	0.088	0.718	0.155	0.739	0.251	0.742	0.405	0.771	0.735	0.819
	FLR	$n \leq 2$	0.126	0.741	0.223	0.765	0.360	0.756	0.581	0.762	1.058	0.765
		$n \geq 3$	0.086	0.725	0.153	0.737	0.247	0.747	0.399	0.768	0.724	0.828
	MSN1+TR	$n \leq 2$	0.173	0.716	0.308	0.743	0.497	0.763	0.807	0.802	1.475	0.705
		$n \geq 3$	0.123	0.743	0.218	0.775	0.353	0.762	0.570	0.764	1.038	0.773
	MSN1+FLR	$n \leq 2$	0.194	0.697	0.344	0.705	0.555	0.697	0.895	0.727	1.604	0.700
		$n \geq 3$	0.121	0.701	0.215	0.727	0.347	0.709	0.561	0.708	1.023	0.738
	MSN2+TR	$n \leq 2$	0.191	0.745	0.339	0.755	0.548	0.750	0.884	0.780	1.586	0.711
		$n \geq 3$	0.146	0.707	0.260	0.733	0.419	0.746	0.678	0.775	1.231	0.709
	MSN2+FLR	$n \leq 2$	0.233	0.696	0.413	0.714	0.665	0.693	1.066	0.627	1.888	0.599
		$n \geq 3$	0.143	0.687	0.253	0.713	0.409	0.717	0.661	0.732	1.199	0.683

damage states (e.g., reduction of severe damage rather than lighter ones, or vice versa). In case the interest was to determine differences in fragility for specific damage states, then the modelling should be carried out with more sophisticated methods (e.g., pushover analysis). For this reason, the fragility model presented in this work is considered reliable for large-scale analyses, rather than for specific and detailed assessments at the scale of individual buildings.

From these results, it is possible to evaluate the overall improvement brought by different interventions and compare the effectiveness of similar interventions applied to different types of buildings. In Fig. 9, the percentage increase of μ calculated for DS3 is shown as an example. From the histograms, on average, MSN interventions are more effective than TR (or CR) and FLR interventions, particularly when applied to Mid-Rise buildings that, due to heavier masses, are subjected to stronger shear actions on the walls. This does not mean that those kinds of interventions (TR or CR) are not effective in general, as their effectiveness in improving the overall behavior and safety level of the building is clear. With this analysis we are addressing effectiveness in terms of damage reduction and, when the out-of-plane collapses of masonry walls are hindered, thanks to the presence of ties or confining elements, then the problem turns into the possible inadequate strength of masonry walls. Hence, the smaller effectiveness of connection elements is due to the fact that, although they bring significant improvements of out-of-plane collapses, however global mechanisms, characterized by the attainment of the masonry wall shear strength, start prevailing. As a result, the overall damage of the building is only slightly improved.

It is also interesting to observe that in historical buildings FLR interventions are more effective than the single intervention of TR. This is due to the fact that a FLR intervention, as it has been conceived in this study, also considers the presence of diffused connections to the walls, thus improving the behavior towards out-of-plane actions, but only from more refined analyses a better seismic load redistribution among walls could emerge. Conversely, in the case of modern (post-1945) buildings, FLR interventions are less effective than CR, and this is very likely due to a combination of various effects, including the better as-built condition of the modern floors, the increase of masses, hence seismic loads, related to the addition of a new collaborating slab, and the more beneficial effect of confining elements, considering the absence or low quality of the existing tie-beams. In the case of interventions on floors of modern buildings, it is even observed a general worsening of the behavior in case of Mid-Rise constructions, probably due to the unfavorable effect of the load increase, not being balanced by a sufficient improvement of stiffness and connections (and of masonry strength).

Lastly, the improvement obtained by the application of combined interventions is not simply the sum of the improvement obtained

Table 6
μ and β values of the as-built and retrofitted fragility models - modern buildings.

			DS1		DS2		DS3		DS4		DS5	
			μ [g]	β [−]	μ [g]	β [−]	μ [g]	β [−]	μ [g]	β [−]	μ [g]	β [−]
1946–1960	AB	$n \leq 2$	0.150	0.732	0.266	0.760	0.430	0.767	0.696	0.783	1.264	0.704
		$n \geq 3$	0.135	0.748	0.240	0.783	0.387	0.782	0.625	0.800	1.134	0.763
	MSN	$n \leq 2$	0.196	0.750	0.348	0.751	0.561	0.732	0.903	0.747	1.618	0.704
		$n \geq 3$	0.189	0.755	0.335	0.761	0.540	0.759	0.873	0.791	1.569	0.714
	CR	$n \leq 2$	0.170	0.800	0.302	0.818	0.488	0.809	0.792	0.820	1.448	0.702
		$n \geq 3$	0.138	0.737	0.244	0.771	0.395	0.775	0.637	0.790	1.157	0.748
	FLR	$n \leq 2$	0.165	0.774	0.293	0.784	0.474	0.787	0.768	0.807	1.403	0.698
		$n \geq 3$	0.133	0.730	0.236	0.764	0.381	0.760	0.616	0.777	1.118	0.753
	MSN+CR	$n \leq 2$	0.227	0.750	0.403	0.754	0.650	0.728	1.042	0.671	1.846	0.643
		$n \geq 3$	0.192	0.759	0.340	0.767	0.549	0.756	0.886	0.778	1.590	0.711
	MSN+FLR	$n \leq 2$	0.230	0.695	0.409	0.716	0.659	0.696	1.057	0.634	1.871	0.608
		$n \geq 3$	0.189	0.689	0.335	0.704	0.541	0.707	0.874	0.753	1.571	0.710
1961–1980	AB	$n \leq 2$	0.208	0.739	0.369	0.741	0.595	0.716	0.956	0.699	1.703	0.679
		$n \geq 3$	0.169	0.676	0.300	0.706	0.485	0.736	0.786	0.785	1.437	0.700
	MSN	$n \leq 2$	0.267	0.754	0.474	0.760	0.766	0.753	1.237	0.659	2.199	0.608
		$n \geq 3$	0.200	0.691	0.354	0.694	0.571	0.680	0.919	0.691	1.644	0.683
	CR	$n \leq 2$	0.245	0.745	0.435	0.751	0.702	0.731	1.127	0.642	1.995	0.602
		$n \geq 3$	0.170	0.688	0.301	0.711	0.487	0.724	0.790	0.760	1.444	0.699
	FLR	$n \leq 2$	0.233	0.689	0.413	0.707	0.665	0.690	1.066	0.627	1.888	0.599
		$n \geq 3$	0.159	0.659	0.283	0.687	0.457	0.702	0.740	0.730	1.348	0.685
	MSN+CR	$n \leq 2$	0.314	0.791	0.556	0.767	0.895	0.756	1.427	0.681	2.451	0.611
		$n \geq 3$	0.207	0.678	0.368	0.689	0.593	0.685	0.953	0.683	1.698	0.671
	MSN+FLR	$n \leq 2$	0.284	0.696	0.504	0.708	0.816	0.714	1.322	0.662	2.368	0.616
		$n \geq 3$	0.196	0.646	0.349	0.657	0.562	0.655	0.906	0.681	1.621	0.682

for the two interventions applied separately, but it is definitely higher, due to the hindrance or delay of different collapse mechanisms, both in- and out-of-plane, and the overall improvement of the building behavior. With reference to the above-mentioned effects of TR and CR on the out-of-plane collapses and on the building damage state in general, it is clear how combining an intervention of TR or CR with the improvement of masonry strength and quality (MSN1, MSN2 or MSN), allows achieving an outcome that is better than the sum of the outcomes of the single interventions carried out separately.

As expected, the improvement in case of modern buildings is generally lower than that of historical buildings, because of the better as-built condition of the former.

As already said, the retrofitted fragility models obtained in this study allow the identification of the overall vulnerability reduction brought by the application of different interventions, but not the variations of individual damage states. More detailed modelling would be required to capture the specific effects of each intervention on the variation of the various damage state, as well as on the overall structural behavior. Since the goal of this work is the assessment of vulnerability reduction at a large scale, such level of detail was not required.

6. Damage maps and results

The mitigated fragility curves presented in the last section can be used to produce seismic damage maps, which can then be compared to the maps elaborated using as-built fragility models. In this work, damage maps have been calculated using the online platform IRMA (Italian Risk Maps), developed by Eucentre (European Center for Training and Research in Earthquake Engineering) under the direction of the Italian Department of Civil Protection [89]. IRMA produces seismic damage and risk maps at municipality level for the entire Italian country by processing information about vulnerability (fragility sets customizable by the user), hazard (Italian Seismic Hazard map - MPS04 [90]) and exposure (from ISTAT census data). IRMA can produce conditional or unconditional damage maps: in this study, unconditional maps were elaborated, which means that all the available return periods of seismic events need to be taken into account, also considering their probability of occurrence within an observation time window. Here, the damage maps have been elaborated for a time window of 50 years. Fig. 10 shows the mean damage maps (for residential masonry residential buildings) for the as-built configuration, obtained by implementing the fragility curves proposed in Ref. [14] in the IRMA platform, as well as for some possible retrofit strategies for which fragility curves have been developed in this study (particularly, Fig. 10 presents the damage maps for TR, MSN2+TR, CR, and MSN + CR). Mean damage maps are calculated as the weighted average of the probability of reaching or exceeding the possible damage levels, according to Equation (1):

$$DS_M = \sum_{i=1}^{5} i \bullet DS_i \tag{1}$$

where DS_M is indeed the mean damage and DS_i represents the probability of reaching a specific damage state i. This indicator provides a synthetic representation of damage that suggests the mean damage that a building would suffer in case of a particular seismic scenario.

The maps shown in Fig. 10 confirm the previous observations, and also point out that, in general, the same intervention leads to

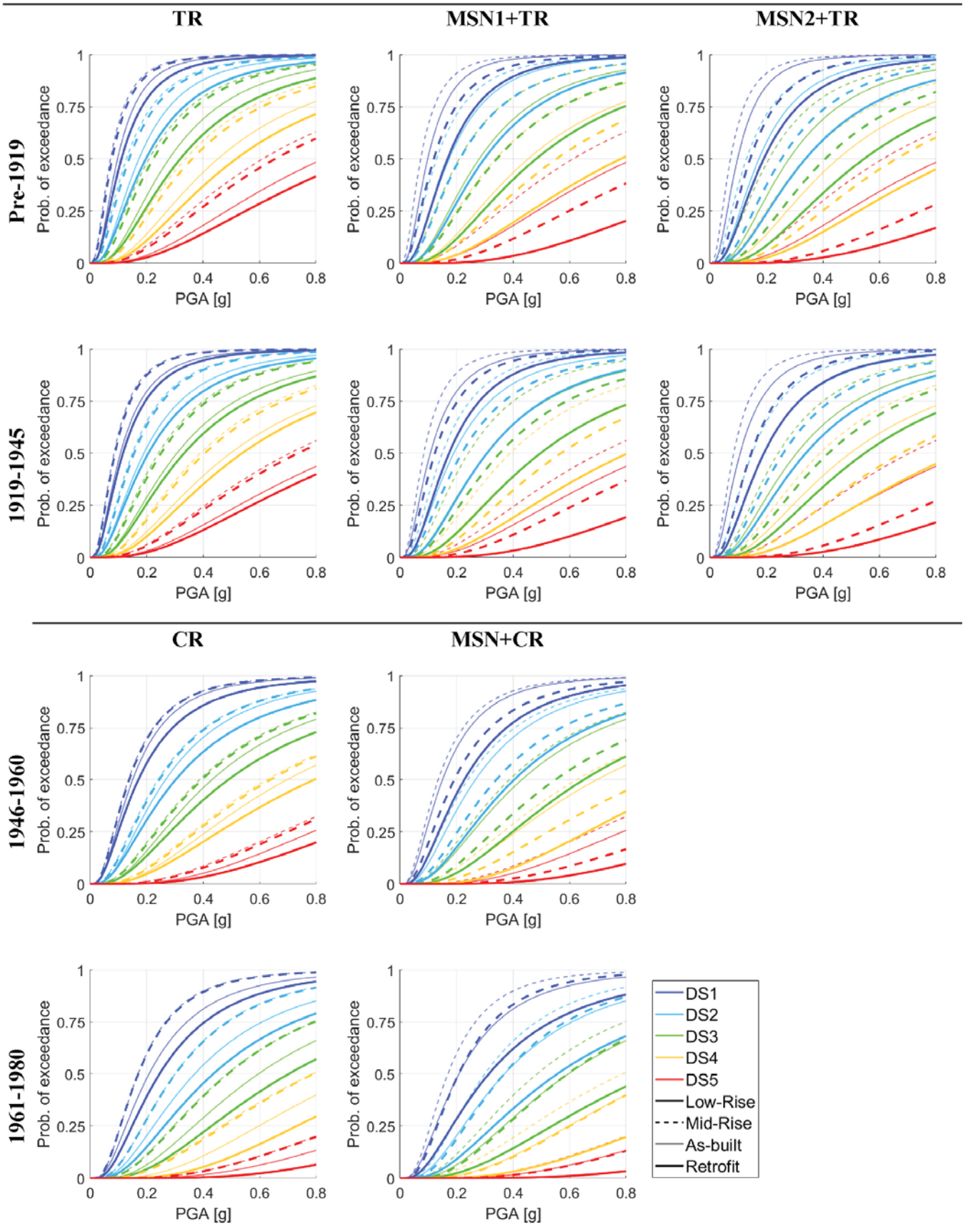

Fig. 7. Mitigated fragility curves for TR, MSN1+TR, MSN2+TR, CR, and MSN + CR.

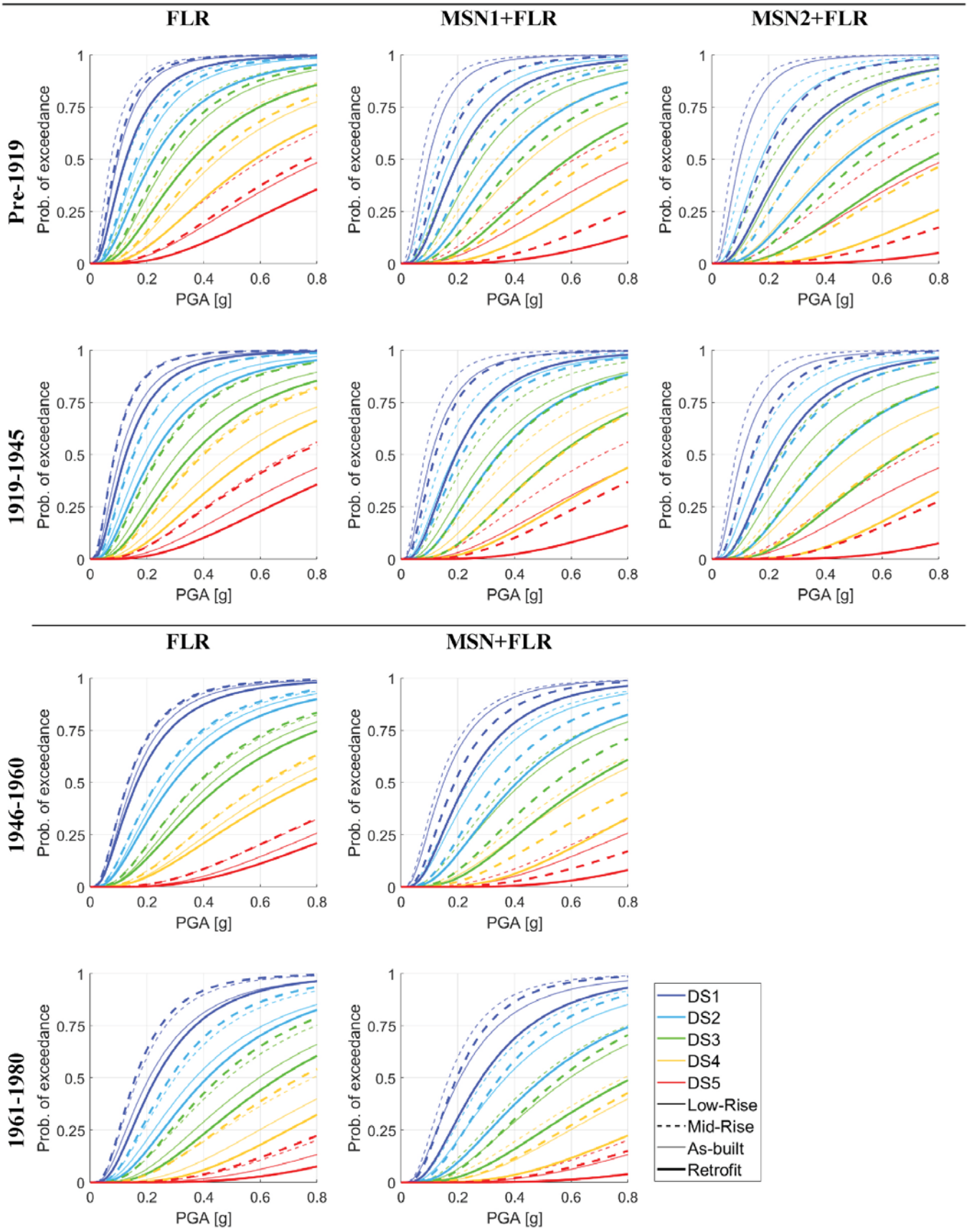

Fig. 8. Mitigated fragility curves for FLR, MSN1+FLR, MSN2+FLR, and MSN + FLR.

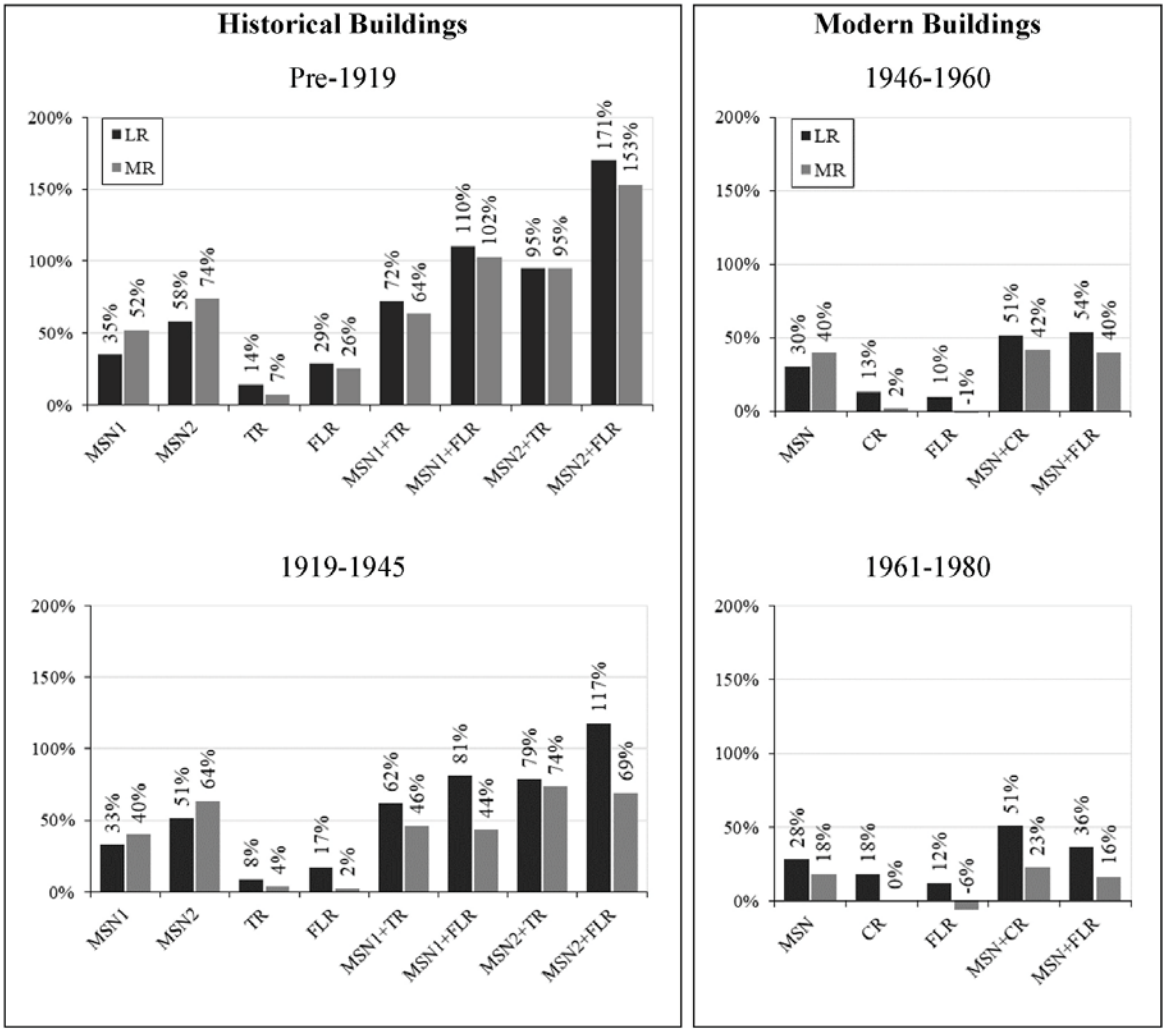

Fig. 9. Percentage of increase of μ calculated for DS3.

greater improvements in areas affected by a higher seismic hazard (i.e., Apennine and North-Eastern areas). This highlights not only the importance and convenience of preventive measures in areas most subjected to earthquakes, but can also give an indication of which intervention can be more suitable for a particular site.

To better visualize this result, it is possible to refer to the graphs of Fig. 11, where the difference between the expected mean damage of the as-built scenario and the expected mean damage of the various retrofit interventions (mean damage variation, Δ_{MD}) is reported for some Italian towns. The towns were chosen to have a good representation of different hazard levels: Table 7 shows the values of ag [g] for the towns considered and for different return periods [90].

Fig. 11 shows how in towns with lower hazard (e.g., Milano), Δ_{MD} is very limited compared to towns with medium or high hazard. Nonetheless, the trend of Δ_{MD} appears to be similar for the various towns, meaning that it is possible to observe a comparable scale factor among different interventions. In addition, it should be noticed that the damage reduction produced by each intervention is very different in towns with a higher hazard level. For example, TR alone in the Pre-1919 epoch produces a very limited mean damage variation, between 0.04 for Milano and 0.18 for L'Aquila, while the same intervention combined with an extensive intervention on masonry (MSN2+TR) produces a variation that goes from 0.25 in Milano to more than one (1.10, that means a complete change of mean damage state) in L'Aquila.

It is also clear how much the different as-built vulnerability influences the efficacy of the various interventions. Indeed, it is possible to obtain a reduction of mean damage up to 1–1.5 DS for historical masonry buildings (particularly in case of Pre-1919 buildings), whereas in the case of more modern buildings, Δ_{DM} almost never exceeds 0.5 DS.

7. Conclusions

This study provides seismic fragility curves for various macro-typologies of Italian residential masonry buildings, derived from a simplified mechanical model. The attention is focused on the effects of different interventions for the improvement of the seismic behavior of masonry buildings belonging to four construction periods, ranging from historical buildings up to buildings designed before the Eighties of the last century, and to two height classes (Low-Rise and Mid-Rise buildings).

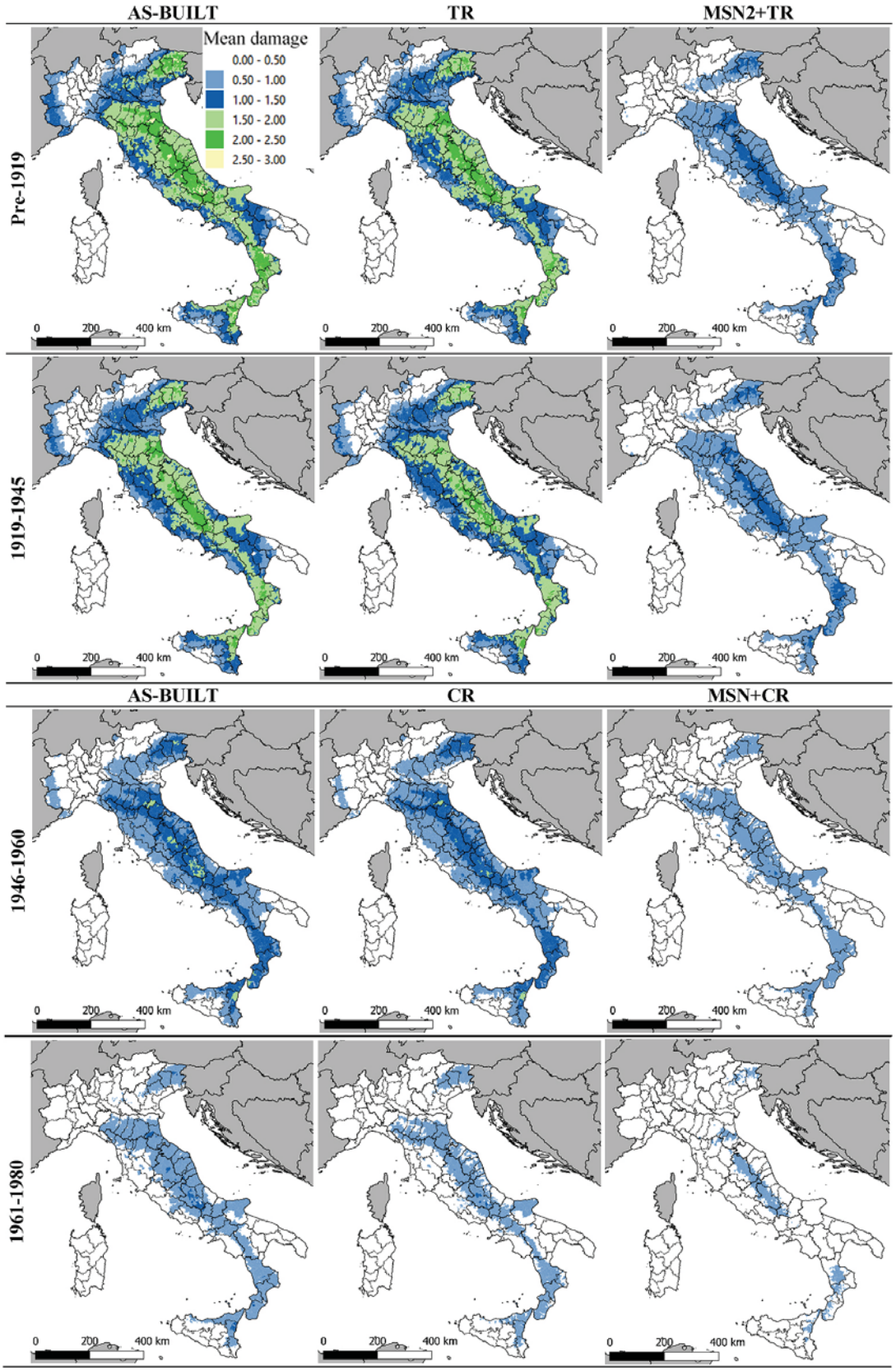

Fig. 10. Mean damage maps for the as-built configuration and some of the investigated interventions (TR, MSN2+TR, CR, and MSN + CR).

Several retrofit interventions have been selected for each construction period, on the basis of the construction features of the buildings, of direct field observations and of experimental studies found in the literature. The software *Vulnus_4.0* was used to produce as-built and retrofitted vulnerability curves of 445 buildings representative of the above-mentioned macro-typologies, and the

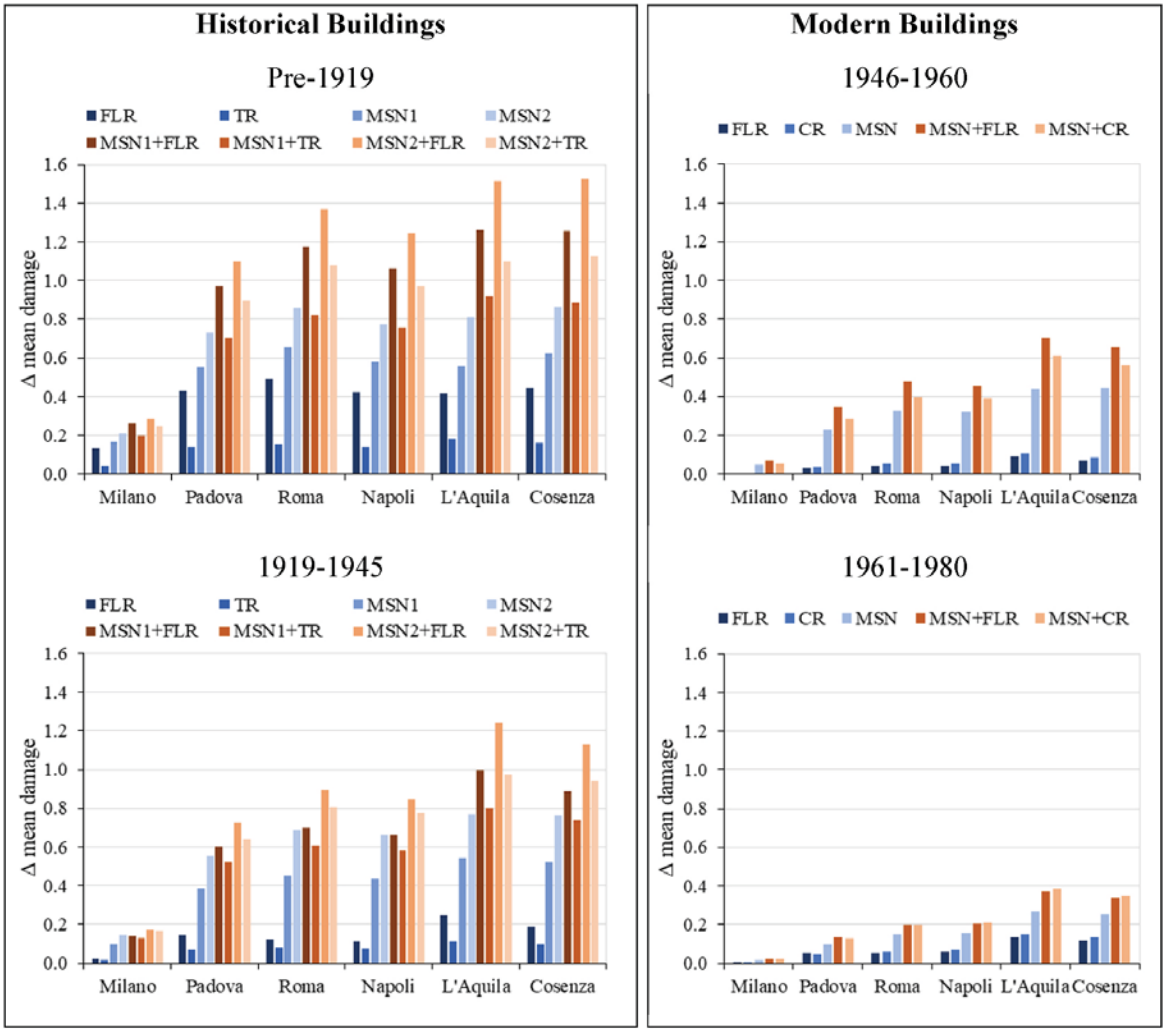

Fig. 11. Δ_{MD} between as-built and retrofitted configurations in different Italian towns.

Table 7
Seismic hazard of some Italian towns expressed in terms of ag [g].

Return period (y)	30	50	72	100	140	200	475	1000	2500
ag [g]									
Milano	0.019	0.024	0.028	0.031	0.035	0.038	0.049	0.059	0.075
Padova	0.030	0.037	0.042	0.048	0.054	0.060	0.082	0.105	0.142
Roma	0.041	0.051	0.059	0.066	0.074	0.083	0.108	0.133	0.172
Napoli	0.045	0.060	0.073	0.086	0.101	0.120	0.168	0.213	0.280
L'Aquila	0.079	0.104	0.123	0.142	0.164	0.191	0.261	0.334	0.452
Cosenza	0.072	0.095	0.114	0.135	0.159	0.188	0.274	0.366	0.514

procedure developed by Donà et al. [14] was followed to create the final fragility sets. Some interventions could be implemented directly in the software, while others were simulated by reproducing their effect on the building behavior. Since the curves produced by *Vulnus_4.0* represent a single damage state (DS2-3), the macroseismic fragility model was calibrated on these curves to represent seismic fragility over five damage states (from DS1 to DS5). The retrofitted fragility model obtained in this study thus describes the overall vulnerability reduction brought by the application of different interventions, rather than the variations of individual damage states, making this model more suitable for large-scale analyses.

Based on the fragility results, some observations on the performance of the implemented interventions were drawn, estimating the vulnerability reduction, in terms of probability of exceedance of damage states, produced by each intervention with respect to the building macro-typology. Mean damage maps have also been produced for Italy, using the IRMA platform, and some analyses on various Italian towns characterized by different seismic hazard have been presented to show the effect of retrofit interventions for areas with different seismic hazard.

The results presented in this paper provide a first step for the analysis of the effectiveness of seismic interventions. When taking into account their costs and their overall impact, it will then be possible to carry out cost-benefit analyses for different risk scenarios and

evaluate the actual effectiveness of different retrofit strategies. These assessments are essential for authorities and risk management stakeholders, as they allow elaborating targeted risk mitigation plans at regional or national level.

Declaration of competing interest

The authors declare that they have no known competing financial interests or personal relationships that could have appeared to influence the work reported in this paper.

Data availability

Data will be made available on request.

Acknowledgements

Special thanks to the Italian Civil Protection Department, which funded this study as part of the ReLUIS-DPC Project 2019–2021 - Work Package 4: MARS (MAps of Risk and Scenarios of seismic damage) - Task 6: Preventive strategies, and ReLUIS-DPC Project 2022–2024 - Work Package 4: MARS-2 (MAps of Risk and Scenarios of seismic damage) - Task 3: Vulnerability. The authors would like to thank the Coordinators of the Project and Work Groups for all the valuable discussions that improved the quality of this study.

References

[1] L. Decanini, A. De Sortis, A. Goretti, R. Langenbach, F. Mollaioli, A. Rasulo, Performance of masonry buildings during the 2002 molise, Italy, earthquake, Earthq. Spectra. 20 (2004) 191–220, https://doi.org/10.1193/1.1765106.
[2] D.F. D'Ayala, S. Paganoni, Assessment and analysis of damage in L'Aquila historic city centre after 6th April 2009, Bull. Earthq. Eng. 9 (2011) 81–104, https://doi.org/10.1007/s10518-010-9224-4.
[3] A. Penna, P. Morandi, M. Rota, C.F. Manzini, F. da Porto, G. Magenes, Performance of masonry buildings during the Emilia 2012 earthquake, Bull. Earthq. Eng. 12 (2014) 2255–2273, https://doi.org/10.1007/s10518-013-9496-6.
[4] L. Sorrentino, S. Cattari, F. da Porto, G. Magenes, A. Penna, Seismic behavior of ordinary masonry buildings during the 2016 central Italy earthquakes, Bull. Earthq. Eng. 17 (2019) 5583–5607, https://doi.org/10.1007/s10518-018-0370-4.
[5] D. Dizhur, S. Wei, M. Giaretton, A.E. Schultz, J.M. Ingham, I. Giongo, Testing of URM wall-to-diaphragm through-bolt plate anchor connections, Earthq. Spectra 37 (2021) 304–323, https://doi.org/10.1177/8755293020944187.
[6] A. Ural, A. Doğangün, H. Sezen, Z. Angın, Seismic performance of masonry buildings during the 2007 Bala, Turkey earthquakes, Nat. Hazards 60 (2012) 1013–1026, https://doi.org/10.1007/s11069-011-9887-4.
[7] G. Vlachakis, E. Vlachaki, P.B. Lourenço, Learning from failure: damage and failure of masonry structures, after the 2017 Lesvos earthquake (Greece), Eng. Fail. Anal. 117 (2020), 104803, https://doi.org/10.1016/j.engfailanal.2020.104803.
[8] N. Augenti, F. Parisi, Learning from construction failures due to the 2009 L'aquila, Italy, earthquake, J. Perform. Constr. Facil. 24 (2010) 536–555, https://doi.org/10.1061/(ASCE)CF.1943-5509.0000122.
[9] M.R. Valluzzi, L. Sbrogiò, Y. Saretta, H. Wenliuhan, Seismic response of masonry buildings in historical centres struck by the 2016 Central Italy earthquake. Impact of building features on damage evaluation, Int. J. Architect. Herit. (2021) 1–26, https://doi.org/10.1080/15583058.2021.1916852.
[10] National Risk Assessment 2018. Overview of the Potential Major Disasters in Italy, DPC - Italian Department of Civil Protection, 2018.
[11] Sendai Framework for Disaster Risk Reduction 2015-2030, United Nations, 2015. https://www.unisdr.org/files/43291_sendaiframeworkfordrren.pdf.
[12] M. Dolce, A. Prota, B. Borzi, F. da Porto, S. Lagomarsino, G. Magenes, C. Moroni, A. Penna, M. Polese, E. Speranza, G.M. Verderame, G. Zuccaro, Seismic risk assessment of residential buildings in Italy, Bull. Earthq. Eng. 19 (2021) 2999–3032, https://doi.org/10.1007/s10518-020-01009-5.
[13] F. da Porto, M. Donà, A. Rosti, M. Rota, S. Lagomarsino, S. Cattari, B. Borzi, M. Onida, D. De Gregorio, F.L. Perelli, C. Del Gaudio, P. Ricci, E. Speranza, Comparative analysis of the fragility curves for Italian residential masonry and RC buildings, Bull. Earthq. Eng. 19 (2021) 3209–3252, https://doi.org/10.1007/s10518-021-01120-1.
[14] M. Donà, P. Carpanese, V. Follador, L. Sbrogiò, F. da Porto, Mechanics-based fragility curves for Italian residential URM buildings, Bull. Earthq. Eng. 19 (2021) 3099–3127, https://doi.org/10.1007/s10518-020-00928-7.
[15] B. Borzi, M. Faravelli, A. Di Meo, Application of the SP-BELA methodology to RC residential buildings in Italy to produce seismic risk maps for the national risk assessment, Bull. Earthq. Eng. 19 (2021) 3185–3208, https://doi.org/10.1007/s10518-020-00953-6.
[16] A. Rosti, C. Del Gaudio, M. Rota, P. Ricci, Paolo, M. Di Ludovico, A. Penna, G.M. Verderame, Empirical fragility curves for Italian residential RC buildings, Bull. Earthq. Eng. 19 (2021) 3165–3183, https://doi.org/10.1007/s10518-020-00971-4.
[17] A. Rosti, M. Rota, A. Penna, Empirical fragility curves for Italian URM buildings, Bull. Earthq. Eng. 19 (2021) 3057–3076, https://doi.org/10.1007/s10518-020-00845-9.
[18] G. Zuccaro, F.L. Perelli, D. De Gregorio, F. Cacace, Empirical vulnerability curves for Italian mansory buildings: evolution of vulnerability model from the DPM to curves as a function of accelertion, Bull. Earthq. Eng. 19 (2021) 3077–3097, https://doi.org/10.1007/s10518-020-00954-5.
[19] S. Lagomarsino, S. Cattari, D. Ottonelli, The heuristic vulnerability model: fragility curves for masonry buildings, Bull. Earthq. Eng. 19 (2021) 3129–3163, https://doi.org/10.1007/s10518-021-01063-7.
[20] G.M. Calvi, R. Pinho, G. Magenes, J.J. Bommer, L.F. Restrepo-Vélez, H. Crowley, Development of seismic vulnerability assessment methodologies over the past 30 years, ISET J. Earthq. Technol. 43 (2006) 75–104.
[21] D. D'Ayala, Assessing the seismic vulnerability of masonry buildings, Handbook of Seismic Risk Analysis and Management of Civil Infrastructure Systems (2013) 334–365, https://doi.org/10.1533/9780857098986.3.334.
[22] V. Manfredi, A. Masi, G. Nicodemo, A. Digrisolo, Seismic fragility curves for the Italian RC residential buildings based on non-linear dynamic analyses, Bull. Earthq. Eng. (2022), https://doi.org/10.1007/s10518-022-01605-7.
[23] S. Ruggieri, M. Calò, A. Cardellicchio, G. Uva, Analytical-mechanical based framework for seismic overall fragility analysis of existing RC buildings in town compartments, Bull. Earthq. Eng. 20 (2022) 8179–8216, https://doi.org/10.1007/s10518-022-01516-7.
[24] 15° censimento della popolazione e delle abitazioni 2011. Website and data warehouse, ISTAT, 2011. https://www.istat.it/it/censimenti-permanenti/censimenti-precedenti/popolazione-e-abitazioni/popolazione-2011.
[25] V. Follador, M. Donà, P. Carpanese, F. da Porto, Fragility curves for Italian residential masonry buildings with retrofit interventions, Proceedings of 8th International Conference on Computational Methods in Structural Dynamics and Earthquake Engineering Methods in Structural Dynamics and Earthquake Engineering (2021) 3083–3097, https://doi.org/10.7712/120121.8698.18819. Athens, Greece.
[26] R. Gentile, C. Galasso, Simplified seismic loss assessment for optimal structural retrofit of RC buildings, Earthq. Spectra 37 (2021) 346–365, https://doi.org/10.1177/8755293020952441.
[27] K. Aljawhari, R. Gentile, C. Galasso, A fragility-oriented approach for seismic retrofit design, Earthq. Spectra 38 (2022) 1813–1843, https://doi.org/10.1177/87552930221078324.

[28] F. da Porto, S. Lagomarsino, S. Cattari, V. Follador, P. Carpanese, M. Donà, S. Alfano, in: Fragility Curves of As-Built and Retrofitted Masonry Buildings in Italy, 3ECEES, 3rd European Conference on Earthquake Engineering and Seismology, Bucharest, Romania, 2022. September 4-9.
[29] M. Donà, P. Carpanese, V. Follador, F. da Porto, Derivation of mechanical fragility curves for macro-typologies of Italian masonry buildings, in: Proceedings of the 7th International Conference on Computational Methods in Structural Dynamics and Earthquake Engineering, Institute of Structural Analysis and Antiseismic Research School of Civil Engineering National Technical University of Athens (NTUA) Greece, Crete, Greece, 2019, pp. 1691–1706, https://doi.org/10.7712/120119.7029.19172.
[30] M. Donà, L. Xu, P. Carpanese, V. Follador, F. Da Porto, L. Sbrogiò, in: Seismic Fragility and Risk of Italian Residential Masonry Heritage, 17th International Brick and Block Masonry Conference (IB2MaC), Krakow, Poland, 2020. July 5-8.
[31] Italian Ministry of Infrastructures, in: Italian (Ed.), DM 1987/11/20 (GU no. 285 of 1987/12/05), Norme Tecniche per la progettazione, esecuzione e collaudo degli edifici in Muratura e per il loro consolidamento, 1987.
[32] A. Bernardini, M. Gori, C. Modena, Application of coupled analytical models and experimental kowledge to seismic vulnerability analyses of masonry buildings, in: Earthquake Damage Evaluation and Vulnerability Analysis of Building Structures, Omega Scientific, Oxon, 1990, pp. 161–180.
[33] M.R. Valluzzi, User Manual of Vulnus_4.0, original program by Bernardini Gori A, Modena R C, Vb version edited by Valluzzi MR, with contributions by Benincà G, Barbetta E, Munari M (2009).
[34] M.R. Valluzzi, V. Follador, L. Sbrogiò, Vulnus Web: a web-based procedure for the seismic vulnerability assessment of masonry buildings, Sustenability (2023) (under revision).
[35] M. Ferrini, A. Melozzi, A. Pagliazzi, S. Scarparolo, Rilevamento della vulnerabilità sismica degli edifici in muratura, Manuale per la compilazione della Scheda GNDT/CNR di II livello (2003).
[36] A. Bernardini, F. Tonon, Aggregation of evidence from random and fuzzy sets, Z. Angew. Math. Mech. 84 (2004) 700–709, https://doi.org/10.1002/zamm.200410145.
[37] G. Grünthal (Ed.), European Macroseismic Scale 1998: EMS-98, European Seismological Commission, Subcommission on Engineering Seismology, Working Group Macroseismic scales, Luxembourg, 1998.
[38] A. Nettis, R. Gentile, D. Raffaele, G. Uva, C. Galasso, Cloud Capacity Spectrum Method: accounting for record-to-record variability in fragility analysis using nonlinear static procedures, Soil Dynam. Earthq. Eng. 150 (2021), 106829, https://doi.org/10.1016/j.soildyn.2021.106829.
[39] F. Jalayer, H. Ebrahimian, A. Miano, G. Manfredi, H. Sezen, Analytical fragility assessment using unscaled ground motion records, Earthq. Eng. Struct. Dynam. 46 (2017) 2639–2663, https://doi.org/10.1002/eqe.2922.
[40] O.C. Celik, B.R. Ellingwood, Seismic fragilities for non-ductile reinforced concrete frames – role of aleatoric and epistemic uncertainties, Struct. Saf. 32 (2010) 1–12, https://doi.org/10.1016/j.strusafe.2009.04.003.
[41] S. Lagomarsino, S. Cattari, Fragility functions of masonry buildings, in: K. Pitilakis, H. Crowley, A.M. Kaynia (Eds.), SYNER-G: Typology Definition and Fragility Functions for Physical Elements at Seismic Risk, Springer Netherlands, Dordrecht, 2014, pp. 111–156, https://doi.org/10.1007/978-94-007-7872-6_5.
[42] C. Margottini, D. Molin, L. Serva, Intensity versus ground motion: a new approach using Italian data, Eng. Geol. 33 (1992) 45–58, https://doi.org/10.1016/0013-7952(92)90034-V.
[43] M. Vettore, Y. Saretta, L. Sbrogiò, M.R. Valluzzi, A new methodology for the survey and evaluation of seismic damage and vulnerability entailed by structural interventions on masonry buildings: validation on the town of castelsantangelo sul nera (MC), Italy, Int. J. Architect. Herit. 16 (2022) 182–207, https://doi.org/10.1080/15583058.2020.1766159.
[44] Y. Saretta, L. Sbrogiò, M.R. Valluzzi, Assigning the macroseismic vulnerability classes to strengthened ordinary masonry buildings: an update from extensive data of the 2016 Central Italy earthquake, IJDRR 62 (2021), 102318, https://doi.org/10.1016/j.ijdrr.2021.102318.
[45] Y. Saretta, L. Sbrogiò, M.R. Valluzzi, Seismic response of masonry buildings in historical centres struck by the 2016 Central Italy earthquake. Calibration of a vulnerability model for strengthened conditions, Construct. Build. Mater. 299 (2021), 123911, https://doi.org/10.1016/j.conbuildmat.2021.123911.
[46] S. Mazzoni, G. Castori, C. Galasso, P. Calvi, R. Dreyer, E. Fischer, A. Fulco, L. Sorrentino, J. Wilson, A. Penna, G. Magenes, 2016–2017 Central Italy earthquake sequence: seismic retrofit policy and effectiveness, Earthq. Spectra 34 (2018) 1671–1691, https://doi.org/10.1193/100717EQS197M.
[47] C. Modena, M.R. Valluzzi, F. da Porto, F. Casarin, Structural aspects of the conservation of historic masonry constructions in seismic areas: remedial measures and emergency actions, Int. J. Architect. Herit. 5 (2011) 539–558, https://doi.org/10.1080/15583058.2011.569632.
[48] Italian Ministry of Infrastructures and Transports. Circolare no. 7 C.S.LL.PP. of 2009/01/21 (GU n.35 del 11-2-2019 - suppl. Ordinario n. 5), Istruzioni per l'applicazione dell'«Aggiornamento delle "Norme tecniche per le costruzioni"» di cui al decreto ministeriale 17 gennaio 2018 (2019) (in Italian).
[49] C. Modena, F. Pineschi, M.R. Valluzzi, Valutazione della vulnerabilità sismica di alcune classi di strutture esistenti, Sviluppo e valutazione di metodi di rinforzo, 2000.
[50] D.V. Oliveira, R.A. Silva, E. Garbin, P.B. Lourenço, Strengthening of three-leaf stone masonry walls: an experimental research, Mater. Struct. 45 (2012) 1259–1276, https://doi.org/10.1617/s11527-012-9832-3.
[51] B. Silva, M. Dalla Benetta, F. da Porto, M.R. Valluzzi, Compression and sonic tests to assess effectiveness of grout injection on three-leaf stone masonry walls, Int. J. Architect. Herit. 8 (2014) 408–435, https://doi.org/10.1080/15583058.2013.826300.
[52] B. Quelhas, L. Cantini, J.M. Guedes, F. da Porto, C. Almeida, Characterization and reinforcement of stone masonry walls, in: A. Costa, J.M. Guedes, H. Varum (Eds.), Structural Rehabilitation of Old Buildings, Springer Berlin Heidelberg, Berlin, Heidelberg, 2014, pp. 131–155, https://doi.org/10.1007/978-3-642-39686-1_5.
[53] E. Vintzileou, A. Miltiadou-Fezans, Mechanical properties of three-leaf stone masonry grouted with ternary or hydraulic lime-based grouts, Eng. Struct. 30 (2008) 2265–2276, https://doi.org/10.1016/j.engstruct.2007.11.003.
[54] A. Kalagri, A. Miltiadou-Fezans, E. Vintzileou, Design and evaluation of hydraulic lime grouts for the strengthening of stone masonry historic structures, Mater. Struct. 43 (2010) 1135–1146, https://doi.org/10.1617/s11527-009-9572-1.
[55] C. Modena, F. Casarin, N. Mazzon, M. Munari, M. Panizza, M.R. Valluzzi, Structural interventions on historical masonry buildings: review of Eurocode 8 provisions in the light of the Italian experience, in: E. Cosenza (Ed.), Eurocode 8 Perspectives from the Italian Standpoint, Doppiavoce, Napoli, Italy, 2009, pp. 225–236.
[56] M. Tomaževič, I. Klemenc, P. Weiss, Seismic upgrading of old masonry buildings by seismic isolation and CFRP laminates: a shaking-table study of reduced scale models, Bull. Earthq. Eng. 7 (2009) 293–321, https://doi.org/10.1007/s10518-008-9086-1.
[57] R. Capozucca, Experimental FRP/SRP–historic masonry delamination, Compos. Struct. 92 (2010) 891–903, https://doi.org/10.1016/j.compstruct.2009.09.029.
[58] A. Borri, G. Castori, M. Corradi, Shear behavior of masonry panels strengthened by high strength steel cords, Construct. Build. Mater. 25 (2011) 494–503, https://doi.org/10.1016/j.conbuildmat.2010.05.014.
[59] CNR-DT 200 R1/2013, Guide for the design and construction of externally bonded FRP systems for strengthening existing structures. Materials, RC and PC structures, masonry structures (2014).
[60] ACI 440.2R-17, Guide for the Design and Construction of Externally Bonded FRP Systems for Strengthening Concrete Structures, ACI, Farmington Hills, MI, USA, 2017, ISBN 9781945487590.
[61] G. de Felice, S. De Santis, L. Garmendia, B. Ghiassi, P. Larrinaga, P.B. Lourenço, D.V. Oliveira, F. Paolacci, C.G. Papanicolaou, Mortar-based systems for externally bonded strengthening of masonry, Mater. Struct. 47 (2014) 2021–2037, https://doi.org/10.1617/s11527-014-0360-1.
[62] M. Corradi, A. Borri, G. Castori, R. Sisti, Shear strengthening of wall panels through jacketing with cement mortar reinforced by GFRP grids, Compos. B Eng. 64 (2014) 33–42, https://doi.org/10.1016/j.compositesb.2014.03.022.
[63] F. da Porto, M.R. Valluzzi, M. Munari, C. Modena, A. Arêde, A.A. Costa, Strengthening of stone and brick masonry buildings, in: A. Costa, A. Arêde, H. Varum (Eds.), Strengthening and Retrofitting of Existing Structures, Springer Singapore, Singapore, 2018, pp. 59–84, https://doi.org/10.1007/978-981-10-5858-5_3.
[64] M. Giaretton, D. Dizhur, E. Garbin, J. Ingham, F. da Porto, In-plane strengthening of clay brick and block masonry walls using textile-reinforced mortar, J. Compos. Construct. 22 (2018), https://doi.org/10.1061/(ASCE)CC.1943-5614.0000866.

[65] CNR-DT 215/2018, Guide for the Design and Construction of Externally Bonded Fibre Reinforced Inorganic Matrix Systems for Strengthening Existing Structures, 2020.
[66] ACI 549.6R-20, Guide to Design and Construction of Externally Bonded Fabric-Reinforced Cementitious Matrix (FRCM) and Steel-Reinforced Grout (SRG) Systems for Repair and Strengthening Masonry Structures, ACI: Farmington Hills,, MI, USA, 2020, ISBN 9781641951203.
[67] M. Valluzzi, L. Sbrogiò, Y. Saretta, Intervention strategies for the seismic improvement of masonry buildings based on FME validation: the case of a terraced building struck by the 2016 Central Italy earthquake, Buildings 11 (2021) 404, https://doi.org/10.3390/buildings11090404.
[68] M. Corradi, A. Borri, E. Poverello, G. Castori, The use of transverse connectors as reinforcement of multi-leaf walls, Mater. Struct. 50 (2017) 114, https://doi.org/10.1617/s11527-016-0977-3.
[69] A. Cascardi, M. Leone, M.A. Aiello, Transversal joining of multi-leaf masonry through different types of connector: experimental and theoretical investigation, Construct. Build. Mater. 265 (2020), 120733, https://doi.org/10.1016/j.conbuildmat.2020.120733.
[70] M. Corradi, C. Tedeschi, L. Binda, A. Borri, Experimental evaluation of shear and compression strength of masonry wall before and after reinforcement: deep repointing, Construct. Build. Mater. 22 (2008) 463–472, https://doi.org/10.1016/j.conbuildmat.2006.11.021.
[71] M.R. Valluzzi, L. Binda, C. Modena, Mechanical behavior of historic masonry structures strengthened by bed joints structural repointing, Construct. Build. Mater. 19 (2005) 63–73, https://doi.org/10.1016/j.conbuildmat.2004.04.036.
[72] M. Tomaževič, M. Lutman, P. Weiss, Seismic upgrading of old brick-masonry urban houses: tying of walls with steel ties, Earthq. Spectra 12 (1996) 599–622, https://doi.org/10.1193/1.1585898.
[73] E. Giuriani, A. Marini, G. Plizzari, Experimental Behavior of Stud Connected Wooden Floors Undergoing Seismic Action/Untersuchung des Verhaltens von mit Bolzen verbundenen Holzdecken unter seismischer Belastung, Restoration of Buildings and Monuments 11 (2005) 3–24, https://doi.org/10.1515/rbm-2005-5924.
[74] A.S. Araújo, D.V. Oliveira, P.B. Lourenço, Numerical study on the performance of improved masonry-to-timber connections in traditional masonry buildings, Eng. Struct. 80 (2014) 501–513, https://doi.org/10.1016/j.engstruct.2014.09.027.
[75] S. Moreira, L.F. Ramos, D.V. Oliveira, P.B. Lourenço, Design parameters for seismically retrofitted masonry-to-timber connections: injection anchors, Int. J. Architect. Herit. 2015 (2015), 15583058, https://doi.org/10.1080/15583058.2015.1113339, 1113339.
[76] C. Calderini, P. Piccardo, R. Vecchiattini, Experimental characterization of ancient metal tie-rods in historic masonry buildings, Int. J. Architect. Herit. 13 (2019) 416–428, https://doi.org/10.1080/15583058.2018.1563230.
[77] E. Cescatti, F. Da Porto, C. Modena, Axial force estimation in historical metal tie-rods: methods, influencing parameters, and laboratory tests, Int. J. Architect. Herit. 13 (2019) 317–328, https://doi.org/10.1080/15583058.2018.1563234.
[78] O. AlShawa, D. Liberatore, L. Sorrentino, Dynamic one-sided out-of-plane behavior of unreinforced-masonry wall restrained by elasto-plastic tie-rods, Int. J. Architect. Herit. 13 (2019) 340–357, https://doi.org/10.1080/15583058.2018.1563226.
[79] S. Podestà, L. Scandolo, Earthquakes and tie-rods: assessment, design, and ductility issues, Int. J. Architect. Herit. 13 (2019) 329–339, https://doi.org/10.1080/15583058.2018.1563239.
[80] F. Graziotti, U. Tomassetti, A. Penna, G. Magenes, Out-of-plane shaking table tests on URM single leaf and cavity walls, Eng. Struct. 125 (2016) 455–470, https://doi.org/10.1016/j.engstruct.2016.07.011.
[81] J.M. Branco, R. Tomasi, Analysis and strengthening of timber floors and roofs, in: A. Costa, J.M. Guedes, H. Varum (Eds.), Structural Rehabilitation of Old Buildings, Springer Berlin Heidelberg, Berlin, Heidelberg, 2014, pp. 235–258, https://doi.org/10.1007/978-3-642-39686-1_8.
[82] M. Piazza, C. Baldessari, R. Tomasi, in: The Role of In-Plane Floor Stiffness in the Seismic Behavior of Traditional Buildings, 14th World Conference on Earthquake Engineering, Beijing, China, 2008. October 12-17.
[83] M.R. Valluzzi, E. Garbin, M. Dalla Benetta, C. Modena, Experimental assessment and modelling of in-plane behavior of timber floors, in: Proceedings of the VI International Conference on Structural Analysis of Historic Construction, vol. 2008, SAHC08, Bath, United Kingdom, 2004, https://doi.org/10.1201/9781439828229. July 2-.
[84] G. Magenes, A. Penna, I.E. Senaldi, M. Rota, A. Galasco, Shaking table test of a strengthened full-scale stone masonry building with flexible diaphragms, Int. J. Architect. Herit. 8 (2014) 349–375, https://doi.org/10.1080/15583058.2013.826299.
[85] I. Senaldi, G. Magenes, A. Penna, A. Galasco, M. Rota, The effect of stiffened floor and roof diaphragms on the experimental seismic response of a full-scale unreinforced stone masonry building, J. Earthq. Eng. 18 (2014) 407–443, https://doi.org/10.1080/13632469.2013.876946.
[86] M.R. Valluzzi, M. Munari, C. Modena, L. Binda, G. Cardani, A. Saisi, Multilevel approach to the vulnerability analysis of historic buildings in seismic areas Part 2: analytical interpretation of mechanisms for vulnerability analysis and structural improvement, Restoration of Buildings and Monuments 13 (2007) 427–442, https://doi.org/10.1515/rbm-2007-6172.
[87] A. Marini, A. Belleri, C. Passoni, F. Feroldi, E. Giuriani, In-plane capacity of existing post-WWII beam-and-clay block floor systems, Bull. Earthq. Eng. 20 (2022) 1655–1683, https://doi.org/10.1007/s10518-021-01301-y.
[88] A. Borri, R. Sisti, M. Corradi, A. Giannantoni, Experimental analysis of masonry ring beams reinforced with composite materials, in: C. Modena, F. da Porto, M. R. Valluzzi (Eds.), Brick and Block Masonry, 0 ed., CRC Press, 2016, pp. 717–726, https://doi.org/10.1201/b21889-90.
[89] B. Borzi, M. Onida, M. Faravelli, D. Polli, M. Pagano, D. Quaroni, A. Cantoni, E. Speranza, C. Moroni, IRMA platform for the calculation of damages and risks of Italian residential buildings, Bull. Earthq. Eng. 19 (2021) 3033–3055, https://doi.org/10.1007/s10518-020-00924-x.
[90] M. Stucchi, C. Meletti, V. Montaldo, H. Crowley, G.M. Calvi, E. Boschi, Seismic hazard assessment (2003-2009) for the Italian building code, Bull. Seismol. Soc. Am. 101 (2011) 1885–1911, https://doi.org/10.1785/0120100130.